Neurochemical Characterization of Brainstem Pro-Opiomelanocortin Cells

Teodora Georgescu,[1,2,4] David Lyons,[1] Barbora Doslikova,[2] Ana Paula Garcia,[2] Oliver Marston,[2] Luke K. Burke,[2] Raffaella Chianese,[1] Brian Y. H. Lam,[3] Giles S. H. Yeo,[3] Justin J. Rochford,[2] Alastair S. Garfield,[2] and Lora K. Heisler[1,2]

[1]Rowett Institute, University of Aberdeen, Foresterhill, Aberdeen AB25 2ZD, UK; [2]Department of Pharmacology, University of Cambridge, Cambridge CB2 1PD, UK; [3]MRC Metabolic Diseases Unit, University of Cambridge Metabolic Research Laboratories, Wellcome Trust-MRC Institute of Metabolic Science, Addenbrooke's Hospital, Cambridge CB2 0QQ, UK; and [4]Centre for Neuroendocrinology & Department of Anatomy, University of Otago, Dunedin 9016, New Zealand

ORCiD number: 0000-0002-4586-8319 (T. Georgescu).

Genetic research has revealed pro-opiomelanocortin (POMC) to be a fundamental regulator of energy balance and body weight in mammals. Within the brain, POMC is primarily expressed in the arcuate nucleus of the hypothalamus (ARC), while a smaller population exists in the brainstem nucleus of the solitary tract ($POMC^{NTS}$). We performed a neurochemical characterization of this understudied population of POMC cells using transgenic mice expressing green fluorescent protein (eGFP) under the control of a POMC promoter/enhancer ($Pomc^{eGFP}$). Expression of endogenous *Pomc* mRNA in the nucleus of the solitary tract (NTS) $Pomc^{eGFP}$ cells was confirmed using fluorescence-activating cell sorting (FACS) followed by quantitative PCR. In situ hybridization histochemistry of endogenous *Pomc* mRNA and immunohistochemical analysis of eGFP revealed that POMC is primarily localized within the caudal NTS. Neurochemical analysis indicated that $POMC^{NTS}$ is not co-expressed with tyrosine hydroxylase (TH), glucagon-like peptide 1 (GLP-1), cholecystokinin (CCK), brain-derived neurotrophic factor (BDNF), nesfatin, nitric oxide synthase 1 (nNOS), seipin, or choline acetyltransferase (ChAT) cells, whereas 100% of $POMC^{NTS}$ is co-expressed with transcription factor paired-like homeobox2b (Phox2b). We observed that 20% of $POMC^{NTS}$ cells express receptors for adipocyte hormone leptin (LepRbs) using a $Pomc^{eGFP}$:$LepRb^{Cre:tdTOM}$ double-reporter line. Elevations in endogenous or exogenous leptin levels increased the in vivo activity (c-FOS) of a small subset of $POMC^{NTS}$ cells. Using ex vivo slice electrophysiology, we observed that this effect of leptin on $POMC^{NTS}$ cell activity is postsynaptic. These findings reveal that a subset of $POMC^{NTS}$ cells are responsive to both changes in energy status and the adipocyte hormone leptin, findings of relevance to the neurobiology of obesity. **(*Endocrinology* 161: 1–13, 2020)**

Key Words: Pomc, leptin receptor, NTS, obesity

The rapid rise in the prevalence of obesity has emphasized the need for a greater understanding of the neurobiological mechanisms that underlie energy homeostasis and body weight. Circulating nutritional cues and neuromodulatory signals are integrated within the brain to regulate energy balance. The central melanocortin system is a critical point of convergence for many of these signals and has a fundamental role in regulating body weight. This pathway is comprised of the endogenous melanocortin agonists derived from POMC, which yield the signaling products α-melanocyte stimulating hormone (α-MSH), β-MSH, γ-MSH, adrenocorticotropic hormone (ACTH), and β-endorphin (1). Brain POMC peptides α-MSH, β-MSH, and γ-MSH compete for action with the endogenous melanocortin

ISSN Online 1945-7170

Received 8 October 2019. Accepted 10 March 2020.
First Published Online 13 March 2020.
Corrected and Typeset 28 March 2020.

receptor antagonist/inverse agonist agouti-related peptide (AgRP) at melanocortin-3 and -4 receptors (MC3R, MC4R) (2), with MC4Rs predominantly linked to energy balance and body weight regulation (3–5). In the adult brain, POMC is expressed in the arcuate nucleus of the hypothalamus ($POMC^{ARC}$) and the brainstem nucleus of the solitary tract ($POMC^{NTS}$) (6, 7). However, during development, POMC is transiently expressed in at least 60 additional brain regions within cells that are not fated to be POMC (8, 9). Accordingly, studies employing $Pomc^{CRE}$ transgenic approaches may involve recombination in off-target sites within the brain and peripheral tissues and should be interpreted accordingly.

Brain infusion of α-MSH or synthetic MC4R agonists reduce food intake and body weight, increase energy expenditure, and improve glucose homeostasis (10–12). Complementing these pharmacological studies, loss-of-function mutations of *Pomc* or *Mc4r*, or over-expression of *Agrp*, promote hyperphagia, obesity, and insulin resistance in multiple species, including zebrafish, mice, dogs, and man, illustrating the strong translational nature of this system (13–23). Furthermore, genetic haploinsufficiency of *Pomc/POMC* in both rodents and humans is associated with preferential over-consumption of dietary fat and increased risk for diet-induced obesity (DIO) (24, 25). The melanocortin system has therefore garnered substantial interest as a potential therapeutic target for obesity and the prevention of type 2 diabetes (T2D) (26, 27).

Though $POMC^{ARC}$ neurons have been well characterized (28, 29), less attention has focused on the smaller population of POMC cells localized in the NTS. $POMC^{NTS}$ neurons are anatomically localized to impact energy homeostasis given that (1) the NTS is a primary integrator of multiple metabolic cues (30–34), and (2) $POMC^{NTS}$ cell activity is modulated in response to the firing of vagal afferent and ingestive-related signals (30, 31, 35). Indeed, chemogenetic activation of $POMC^{NTS}$ neurons results in a suppression of feeding and an enhancement of short-term satiety (36). A recent report indicated that $POMC^{NTS}$ is required for the acute anorectic effect of obesity medication 5-HT_{2C}R agonist lorcaserin (37). However, what has not been established is whether other neuropeptides/neurotransmitters implicated in energy homeostasis are co-expressed with $POMC^{NTS}$ and the direct endogenous regulators of $POMC^{NTS}$ neuron activity.

Specifically, the NTS contains other appetite-regulating neuropeptides and neurotransmitters such as cholecystokinin (CCK) (38, 39), glucagon like peptide-1 (GLP-1) (40, 41), catecholamines (39, 42), brain-derived neurotrophic factor (BDNF) (43), and nesfatin (44). Previous reports indicate that receptors (LepRbs) for the adipocyte hormone leptin are co-expressed with a subset of $POMC^{NTS}$ neurons using a $Pomc^{GFP}$ mouse line (43, 45), though others have not found evidence for this using a $Pomc^{CRE}$ line (46). In both mice and humans, the absence of *LepRb/LEPRB* leads to morbid obesity, hyperphagia, insulin resistance, and decreased energy expenditure, amongst other symptoms (47–49). Illustrating that the specific subset of LepRb co-expressed with brain POMC is involved in this metabolic phenotype, selective inactivation of LepRb only in POMC cells produces a milder version of this phenotype (50, 51). However, this Cre/Lox approach does not distinguish between LepRbs expressed within POMC in the ARC or NTS. Here we aimed to clarify the distribution, neurochemical identify, and leptin responsiveness of $POMC^{NTS}$.

Material and Methods

Animals

Male and female *Pomc-enhanced green florescent protein* ($Pomc^{eGFP}$; kindly provided by Prof. Richard Simerly and Prof. Malcolm Low) (52), *LepRb-Ires-Cre::Rosa26-eGFP* ($LepRb^{CRE:eGFP}$) (53) and *LepRb-Ires-Cre:tdTOMATO* ($LepRb^{tdTOM}$; kindly provided by Prof. Joel Elmquist and Prof. Jeffrey Friedman) (54) mice were used. A $Pomc^{eGFP}$:$LepRb^{tdTOM}$ double-reporter line was produced by crossing homozygous $Pomc^{eGFP}$ and $LepRb^{tdTOM}$ mice. All mice were maintained on a 12-hour light, 12-hour dark cycle with *ad libitum* access to a standard laboratory chow diet and water unless indicated otherwise. All procedures performed were in accordance with the UK Animals (Scientific Procedures) Act, 1986 and with appropriate ethical approval.

Immunofluorescent histochemistry

Mice were deeply and terminally anesthetized with pentobarbitone (50 mg/kg i.p.) and transcardially perfused with diethylpyrocarbonate (DEPC)-treated phosphate buffered saline (PBS) followed by 10% neutral buffered formalin (Sigma-Aldrich, Gillingham, UK). Brains were extracted, postfixed in 10% neutral buffered formalin for up to 6 hours, and then cryoprotected through emersion in a 20% sucrose solution in PBS for 1–2 days at 4°C. Brains were sectioned at 25 µm on a freezing sliding microtome and collected in 5 equal series.

Free-floating NTS sections were washed in PBS and incubated for 1 hour with blocking buffer (2% bovine serum albumin with 0.25% Triton X-100 in PBS). Sections were then incubated overnight at 4°C in blocking buffer with a primary antibody: chicken anti-GFP (1:500, Abcam, Cambridge, UK [RRID: AB_300798 (55)]), rabbit anti-mCherry (1:1000, Rockland Immunochemicals, Limerick, PA [RRID: AB_2614470 (56)]), rabbit antinesfatin (1:1000, Phoenix Pharmaceuticals, Burlingame, CA [RRID: AB_2737429 (57)]), mouse antityrosine hydroxylase (TH; 1:1000, Chemicon, Temecula, CA [RRID: AB_390204 (58)]), goat anticholine

acetyltransferase (ChAT; 1:1000, Millipore, Billerica, MA [RRID: AB_2079751 (59)]), rabbit antinitric oxide synthase (nNOS; 1:1000, Immunostar, Hudson, WI [RRID: AB_572255 (60)]), rabbit antiseipin antibody (1:1000, Dr. D. Ito, Keio University School of Medicine, Japan (61, 62) [RRID: AB_2819210 (63)]), and rabbit antipaired-like homeobox 2b (Phox2b; 1:1000, Abcam, Cambridge, UK [RRID: AB_10675986 (64)]). The tissue was subsequently washed in PBS and incubated for 1 hour with the corresponding secondary Alexa Fluor antibodies (1:500, ThermoFisher, Paisley, UK [RRID: AB_2340375 (65), RRID: AB_141637 (66), RRID: AB_141633 (67), RRID: AB_142540 (68)]). Sections were mounted onto microscope slides and visualized under an Axioskop II microscope (Carl Zeiss, Oberkochen, Germany) and images were taken with an AxioCam (Carl Zeiss, Oberkochen, Germany) digital camera. Sections containing the NTS were assigned a bregma level and boundaries of the NTS delineated based on neuroarchitecture and a mouse brain atlas (69). The number of *Pomc*^{eGFP} immunoreactive (IR) cells, neurochemically defined cells, and double-labeled cells falling within the defined regions were counted and expressed as a percentage of total POMC-eGFP-IR expressing cells in that brain slice.

cFOS immunohistochemistry

Pomc^{eGFP} mice were injected with mouse recombinant leptin (5 mg/kg, i.p., Merck, Whitehouse Station, NJ) or vehicle during the light cycle and food was removed. Two hours later, mice were deeply anesthetized with pentobarbitone (50 mg/kg i.p.) and transcardially perfused with DEPC-treated PBS followed by 10% neutral buffered formalin. Another cohort of *Pomc*^{eGFP} mice were fed ad libitum (n = 4), 12-hour fasted overnight (n = 5) or 12-hour fasted overnight followed by a 2-hour light cycle refeeding (n = 5). Mice were then injected with deep terminal anesthesia and transcardially perfused with DEPC-treated PBS followed by 10% neutral buffered formalin. Brains were extracted and tissue prepared as described above. Free-floating NTS sections were processed at room temperature. Tissue was washed in PBS and then treated for 30 minutes with 0.3% H_2O_2 in PBS. Tissue was then washed in PBS, blocked for 1 hour in blocking solution (0.25% Triton X-100 and 3% normal donkey serum in PBS) and incubated overnight in primary antibody rabbit anti-c-fos added to blocking solution (cFOS; 1:5000, Calbiochem, Watford, UK [RRID: AB_2106755 (70)]). The sections were next incubated in biotinylated donkey antirabbit IgG (1:1000, Jackson ImmunoResearch Laboratories, West Grove, PA [RRID: AB_2340593 (71)]) for 1 hour, followed by 2-hour incubation in an avidin–biotin complex solution (1:500, Vectastain Elite ABC Kit, Vector Laboratories, Peterborough, UK) diluted in PBS. After several washes in PBS, sections were incubated in a solution of 0.04% diaminobenzidine tetrahydrochloride (DAB) and 0.01% H_2O_2 in PBS. Brain tissue was then processed for GFP immunofluorescent histochemistry (IHC) and analyzed as described above. Quantitative analysis of dual-labeled cells was expressed as a percentage of the total number of POMC-eGFP-IR positive cells.

In situ hybridization histochemistry and IHC

In situ hybridization histochemistry (ISHH) was conducted as previously described (43). Briefly, mice were injected with deep terminal anesthesia and transcardially perfused with DEPC-treated PBS followed by 10% neutral buffered formalin. Brains were extracted and tissue prepared as described above. Radiolabelled riboprobes specific to the mRNA sequences of POMC, PPG, BDNF, and CCK were used to detect gene expression. Linearized recombinant plasmids were subjected to in vitro transcription with a T7 RNA polymerase (Ambion Inc., Austin, TX) in the presence of ^{35}S-labeled UTP. cRNA riboprobes were diluted to 2 × 10^7 cpm/ml in a hybridization solution. ^{35}S-labeled *Pomc* was examined within adjacent brainstem sections ranging from -6.36 to -8.24 from bregma of 2- to 6-month-old male and female wild type C57BL/6 (n = 7) and *Pomc*^{eGFP} (n = 7) mice. Sections mounted onto microscope slides were placed with Carestream Kodak Biomax MR single emulsion film (Sigma) in a light tight box for 5 days. Films were scanned and manually analyzed, confirming ^{35}S *Pomc* within the NTS. High-resolution images were generated using an AxioCam HRc (Carl Zeiss) interface with a brightfield Axioskop II microscope (Carl Zeiss).

Following ISHH, free-floating tissue processed for dual-histochemical staining was washed in PBS before commencement of the IHC protocol. Sections were treated for 30 minutes in 0.3% H_2O_2 in PBS, rinsed in PBS, and blocked in 0.5% BSA/0.5% TritonX-100 in PBS for 1 hour. Sections were incubated in blocking buffer containing goat anti-GFP antibody (1:1000, Abcam, Cambridge, UK [RRID: AB_304897 (72)]) overnight. Sections were washed in PBS and a biotinylated rabbit antigoat secondary antibody (1:1000, Vector Laboratories, Peterborough, UK [RRID: AB_2336126 (73)]) in blocking buffer for 1 hour. Sections were then washed in PBS and incubated for 1 hour in VectaStain ABC reagent and chromogenic detection was conducted using DAB reagent (Vector Laboratories, Peterborough, UK). Sections were mounted onto microscope slides and air dried. Slides were dipped in photographic emulsion (Kodak, Rochester, NY) and stored at 4°C for 2 weeks before being developed in D-19 developer and fixer (Kodak). Double-labeled cells were recorded if GFP-IR-positive cell bodies contained overlying black grains that were in a quantity greater than 3 times the background and conformed to the shape of the GFP-IR cell bodies.

Isolation of NTS POMC-GFP cells with FACS

Four-week-old male and female ad libitum–fed *Pomc*^{eGFP} mice (n = 6) were sacrificed between 9:00 and 10:00 AM. The NTS was microdissected into ice cold dissociation buffer consisting of 0.36% glucose (Sigma, Gillingham, UK), 2 × 10^{-4}% phenol red solution (Sigma), and 1 mM HEPES buffer (Sigma) in HBSS solution (Invitrogen, Paisley, UK). 10X Ky/Mg solution consisting of 0.19% kynurenic acid (Sigma), 5 × 10^{-4}% phenol red solution (Sigma), 5 mM HEPES buffer (Sigma), and 0.1M $MgCl_2$ (Sigma), pH 7.5, was added before use. Dissociation media was replaced with 1 ml prewarmed 20 U/ml papain solution consisting of 20X L-cysteine solution (Sigma), papain solution (Sigma), and dissociation

medium (containing 10X Ky/Mg) and nuclei were incubated at 37°C for 30 minutes. Papain solution was replaced with 1 ml prewarmed 10 mg/ml trypsin inhibitor solution (Sigma, diluted in dissociation media) and the nuclei incubated at 37°C for 10 minutes. Trypsin inhibitor was removed and nuclei were washed with 1 ml ice cold PBS (Sigma) with 2% FCS (P.A.A. laboratories, Ltd., Yeovil, UK). Phosphate buffered saline was replaced with 2 ml PBS with 2% FCS and the solution triturated. Samples were filtered through a 70 µm cell strainer (BD Falcon, Tewksbury, MA). Fluorescence-activating cell sorting was performed using an Influx Cell Sorter (BD Biosciences, San Jose, CA) utilizing a previous established method (31, 32). Cell gating was set according to cell size (FSC), cell granularity (SSC), FSC pulse-width for singlets, and fluorescence at 488 nm/532 nm for GFP and 647/670 nm for nuclear stain with DraQ7 (Biostatus, Shepshed, Leicester, UK). Pools of GFP-positive (GFP+) and GFP-negative (GFP-) cells were sorted into a plate containing RLT lysis buffer (Qiagen, Manchester, UK) and RNA was isolated using RNeasy Plus Micro Kit (Qiagen). Reverse transcription and whole transcriptome amplification were performed using Nugen Ovation Pico WTA system V2 following the manufacturer's instructions. *Pomc* expression was determined by quantitative real-time PCR (qPCR) using Sybr green with primers designed specifically for *Pomc* (Forward CTCCTGCTTCAGACCTCCAT, Reverse-TTTTCAGTCAGGGGCTGTTC), *Gfp* (Forward- AGCCGCTACCCCGACCACAT, Reverse- CGGTTCACCAGGGTGTCGCC). Gene expression was normalised to *Gapdh* (Forward- TGTTCCTACCCCCAATGTGT, Reverse-GGTCCTCAGTGTAGCCCAAG) in the same samples.

Electrophysiology

Standard current and voltage clamp whole-cell patch clamp electrophysiology recordings were made from POMC^{NTS} cells. Specifically, *Pomc*^{eGFP} mice (6–10 weeks old) were injected with a terminal dose of pentobarbitone (50 mg/kg, i.p.), decapitated, brains rapidly extracted, and immediately submerged in an ice-cold solution containing 250 mM sucrose, 2.5 mM KCl, 21 mM $NaHCO_3$, 1.2 mM NaH_2PO_4, 3 mM glucose, 4 mM $MgCl_2$, and 0.1 mM $CaCl_2$ bubbled with 5% CO_2 and 95%O_2. The brain was fixed to a vibrating microtome (Slicer HR2; Sigmann Elektronik, Hüffenhardt, Germany) and 180 µm coronal sections of the brainstem containing the NTS were prepared. The slices were then incubated for 25 minutes at 34°C in oxygenated artificial cerebral spinal fluid (aCSF) containing 125 mM NaCl, 2.5 mM KCl, 21 mM $NaHCO_3$, 1.2 mM NaH_2PO_4, 3 mM glucose, 2 mM $MgCl_2$, and 2 mM $CaCl_2$. Prior to recording, slices were allowed to recover in the aCSF solution at room temperature for a minimum of 1 hour. Green fluorescent protein cells in live slices were identified using a Nikon Eclipse E6000FN microscope fitted with an LED light source (Cairn, Edinburgh, UK). During recording, unless otherwise described, slices were continuously perfused at a rate of ca. 2 ml/min with oxygenated aCSF solution at 31°C. Leptin was bath applied. Thick-walled glass pipettes (Harvard Apparatus, Holliston, MA) of 4 to 5 MΩ resistance were pulled using a Zeitz DMZ micropipette puller (Zeitz Instruments GmbH, Martinsried, Germany). Pipettes were filled with the following intracellular solution: 120 mM K-gluconate, 10 mM KCl, 0.1 mM EGTA, 10 mM HEPES, 4 mM K_2ATP, and 1 mM Na_2ATP at pH 7.3 (with KOH). Recordings were performed using an EPC10 amplifier and Patchmaster software (HEKA, Lambrecht/Pfalz, Germany). Where indicated, the following combination of neurotransmission inhibitors was used: 1 µM tetrodotoxin (TTX), 3 µM strychnine, 50 µM picrotoxin, 50 µM D-AP5, 10 µM CNQX. Liquid junction potential was 10 mV and not compensated. The recorded current was sampled at 10 kHz and filtered at 5 kHz unless otherwise stated. No effect was set as a change in membrane potential less than 2 mV. All compounds were dissolved in water with the exception of picrotoxin, which was dissolved in ethanol.

Leptin ELISA

Animals were terminally anesthetized with pentobarbitone (50 mg/kg, i.p.). The blood was collected in EDTA-coated tubes (Startedt AG & Co., Numbrecht, Germany). To separate plasma, whole blood was centrifuged at 3500 rpm for 15 minutes at 4°C. Leptin concentrations in serum samples was determined using Mouse Leptin Quantikine® ELISA (R&D Systems, Abington, UK) according to the manufacturer's protocol at room temperature. Briefly, the kit equilibrated for 30 minutes at room temperature. Assay diluent RD1W (50 µl) and sample (50 µl) were added to the 96-well microplate. Next, working leptin standards and leptin controls were added and the plate was covered for 2 hours. Each well was aspirated and washed (5x) with 400 µl wash buffer. Mouse leptin conjugate (100 µl) was added to each well and the plate was incubated for 2 hours. The washing step was repeated. Substrate solution (100 µl) was added to each well and the plate, and the plate was covered to protect it from light exposure and left for 30 minutes. Finally, the reaction was stopped by adding 100 µl of stop solution, initiating a color change from blue to yellow. The plate was mixed by gentle tapping and the absorbance was then measured within 30 minutes on an EnVision® 2104 Multilabel Plate Reader (Perkin Elmer, Waltham, MA), measuring the absorbance at 450 nm and subtracting the absorbance at 540 nm/570 nm. The serum leptin levels in each group were determined using the standard curve obtained from the leptin standards provided.

Statistics

Data were analyzed with t-test or one-way ANOVA followed by Tukey's post hoc tests, where appropriate. For all analyses, significance was assigned at $P < 0.05$. Data are presented as mean ± SEM.

Results

Pomc mRNA and Pomc^{eGFP} distribution in the NTS

POMC is an essential regulator of energy homeostasis and body weight, and POMC neurons within the ARC have been well characterized (28, 29). POMC cells

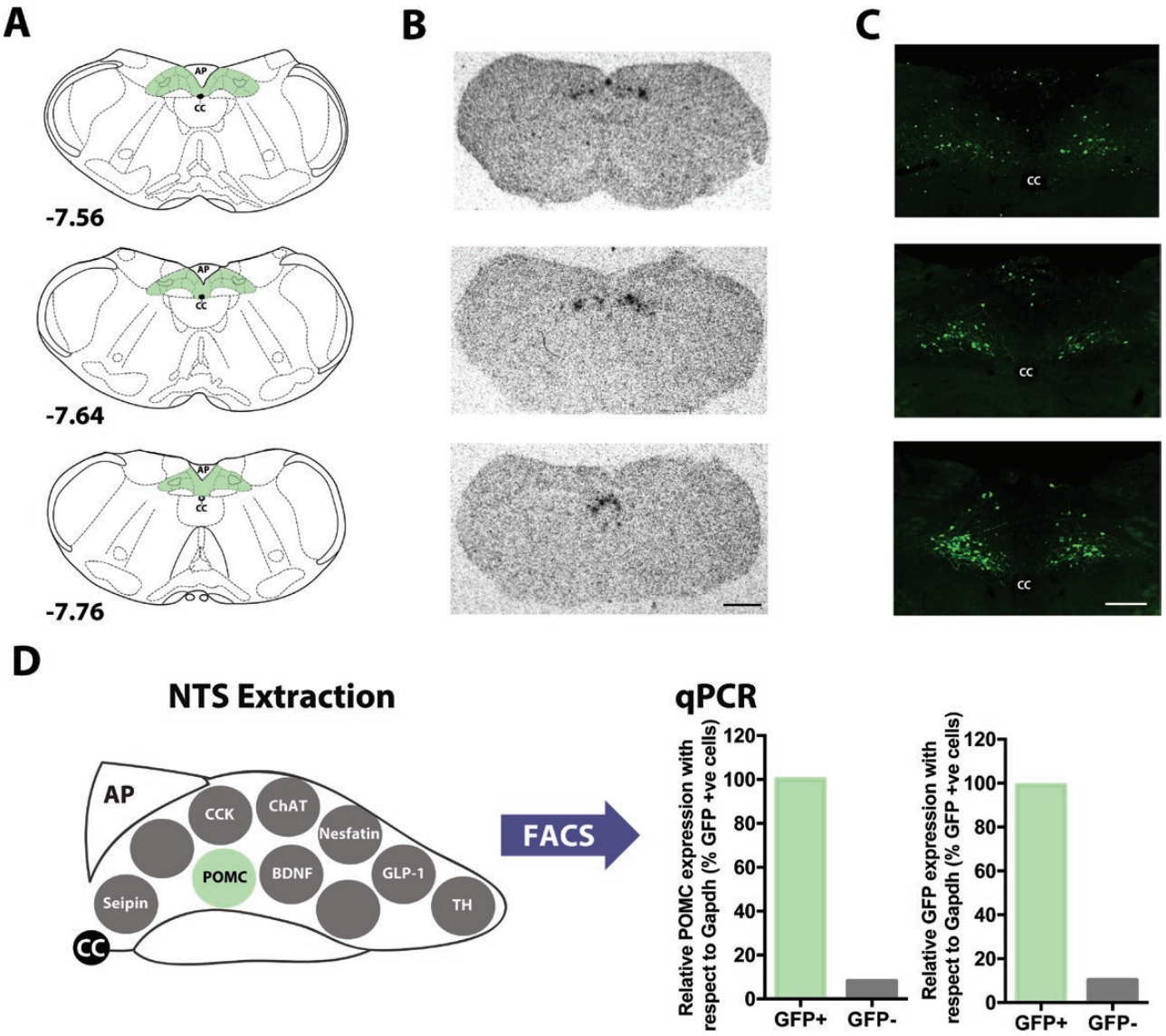

Figure 1. POMC^{NTS} expression and *Pomc*^{eGFP} validation. **A:** Adapted brain atlas (69) schematics of NTS (shaded green area) at -7.56 to -7.76 from bregma. **B:** In situ hybridization histochemistry (ISSH) with a ^{35}S-labelled *Pomc* riboprobe revealed the highest level of *Pomc* mRNA (black grains) within the NTS is between -7.5 to -7.8 from bregma in adult wild-type C57BL/6 mice (n = 7). These findings were reproduced in *Pomc*^{eGFP} mice (n = 7). **C:** Representative photomicrographs of GFP immunofluorescence (IF) in adult male and female *Pomc*^{eGFP} mice (n = 20) also identified that the most abundant distribution of GFP-IR cells is between -7.5 to -7.8 from bregma**. D:** Expression of *Pomc* mRNA in GFP cells in extracted NTS of *Pomc*^{eGFP} mice was confirmed using fluorescence-activating cell sorting (FACS) followed by qPCR analysis. *Pomc* and *Gfp* mRNA were normalized to that of the housekeeping gene *Gapdh*. Expression of *Pomc* and *Gfp* mRNA is expressed as a percentage of that determined in GFP-positive (GFP+) cells and compared to GFP-negative (GFP-) cells. CC, central canal, scale bar B 500 µm; scale bar C 125 µm.

are also localized within the NTS. Using in situ hybridization with a ^{35}S *Pomc* riboprobe, endogenous *Pomc* mRNA expression was visualized within the NTS of wild-type male and female mice on a C56BL/6 background (n = 7) and *Pomc*^{eGFP} mice (n = 7). ^{35}S *Pomc* within the NTS was most abundant between -7.5 to -7.8 from bregma (Fig. 1A and 1B). Scattered cells were also evident at more rostral and caudal levels. POMC^{NTS} has likely received less attention compared to POMC^{ARC} because this NTS subpopulation is smaller and more difficult to visualize on a single cell level with standard histochemical techniques, as we have observed here. To overcome these technical difficulties we employed a *Pomc*^{eGFP} reporter mouse line to map the distribution of individual POMC cells within the brainstem. Expression of GFP protein confirmed that the majority of brainstem POMC cells sit within caudal NTS (-7.5 to -7.8 from bregma; Fig. 1C).

NTS validation of *Pomc*^{eGFP} mouse line

To confirm the expression of *Pomc* mRNA within eGFP cells, the NTS was microdissected from *Pomc*^{eGFP} mice (n = 6), and FACS followed by *Pomc* and *Gfp* qPCR was performed (Fig. 1D). One-hundred percent

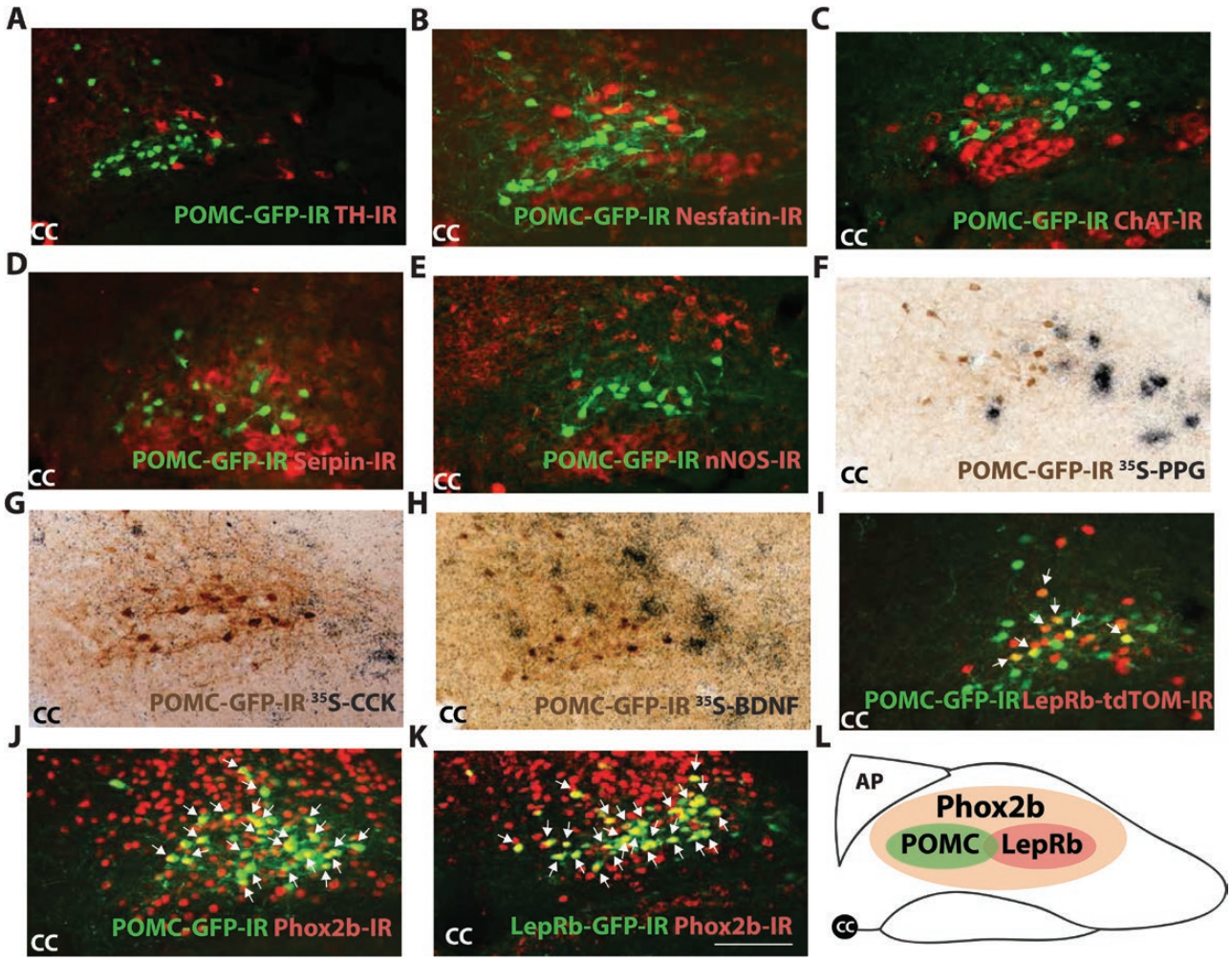

Figure 2. Neurochemical characterization of POMC^{NTS} neurons. Immunohistochemical analysis of adult male and female *Pomc*^{eGFP} mice demonstrated GFP-IR cells (green) to be negative for catecholamine cell marker tyrosine hydroxylase (TH)-IR (red) **(A)**, nesfatin-IR (red) **(B)**, acetylcholine cell marker choline acetyltransferase (ChAT)-IR (red) **(C)**, protein seipin-IR (red) **(D)** and enzyme nitric oxide synthase 1 (nNOS)-IR (red) (n = 3–5 mice per analysis) **(E)**. Dual IHC and ISHH analysis of adult male and female *Pomc*^{eGFP} mice demonstrated the absence of GFP-IR co-expression (brown cytoplasmic stain) with ^{35}S *preproglucagon* (*Ppg*) **(F)**, ^{35}S *cholecystokinin (Cck)* **(G)** or ^{35}S *brain derived neurotrophic factor* (*Bdnf*) mRNA (black grains) (n = 3–5 mice per analysis) **(H)**. **I:** Double-IF analysis in adult male and female *Pomc*^{eGFP}*:LepRb*$^{Cre:tdTomato}$ mice (n = 9) revealed a subset of POMC-expressing neurons (green) were co-expressed with LepRb-expressing cells (red). **J:** In *Pomc*^{eGFP} mice (n = 4) and *LepRb*$^{CRE:eGFP}$ mice (n = 4) **(K)**, all GFP-IR cells (green) were Phox2b-IR positive (red). **L:** Schematic illustrating overlap of POMC, Phox2b, and LepRb in the NTS. Level of NTS presented in **(A–K)**, -7.56 to -7.76 from bregma. Arrows represent dual-labeled cells. CC, central canal; scale bar, 50 µm applies to **(A–K)**.

of GFP-positive cells expressed *Pomc* mRNA as compared to 8% of GFP-negative cells. Similarly, 99% of GFP-positive cells expressed *Gfp* mRNA as compared to 10% of GFP-negative cells. These data provide the first NTS validation of the *Pomc*^{eGFP} line and verify the expression of endogenous POMC^{NTS}.

Neurochemical characterization of POMC^{NTS} neurons

The NTS has a regulatory role in a large number of physiological processes. As a consequence of this functional heterogeneity, this nucleus is home to numerous distinct neuronal populations. To characterize POMC^{NTS} cells, we examined the level of co-expression between *Pomc*^{eGFP} and other neurochemicals and receptors implicated in the regulation of energy balance. We observed that POMC^{NTS} cells do not co-localize with catecholamines epinephrine or norepinephrine using TH to visualize this subset of cells (Fig. 2A). Similarly, *Pomc*^{eGFP} was not co-expressed with the neuropeptide nesfatin-1 (Fig. 2B) or the neurotransmitter acetylcholine using choline acetyltransferase (ChAT; Fig. 2C). *Pomc*^{eGFP} was expressed in a distinct population to the protein seipin associated with lipodystrophy (Fig. 2D) and the enzyme nitric oxide synthase 1 (nNOS; Fig. 2E). Likewise, *Pomc*^{eGFP} was not co-localized with neuropeptides involved in the reduction of food intake, preproglucagon (PPG)/GLP-1

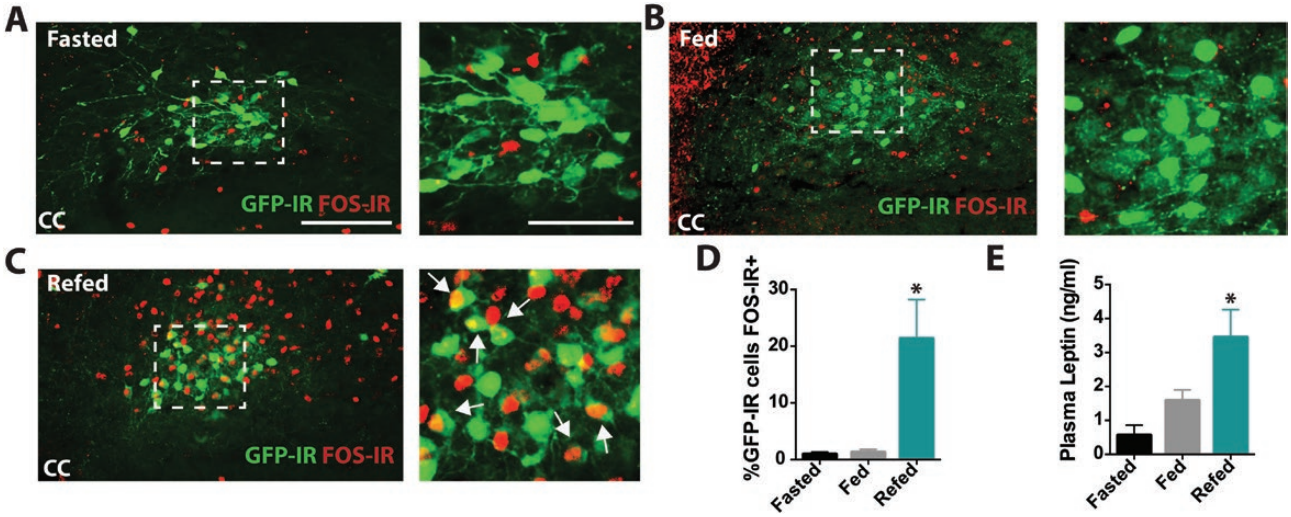

Figure 3. *Pomc*^{eGFP} cells increase their activity in response to food intake. **A-D:** *Pomc*^{eGFP} mice exhibit more FOS-IR in GFP-IR cells within the NTS in response refeeding compared to cells from mice in the ad libitum–fed or 12-hour fasted state (n = 4–5). **E:** Endogenous plasma leptin levels are increased following refeeding (n = 8) compared to ad libitum–fed (n = 9) or 12-hour fasted mice (n = 4) as measured by an ELISA assay. Level of NTS presented in **(A–C)**, -7.76 from bregma. Arrows represent dual-labeled cells. CC, central canal. Scale bar, 50 µm applies to **(A–C)**. Scale bar in inset, 25 µm. Data are presented as mean ± SEM, * $P < 0.05$.

(Fig. 2F), CCK (Fig. 2G), or BDNF (Fig. 2H), as revealed with immunohistochemistry combined with in situ hybridization. Thus, *Pomc*^{eGFP} neurons appear to reside in a distinct subgroup within the NTS and do not co-express other well-characterized regulators of energy homeostasis.

We then examined potential endogenous regulators of POMC^{NTS}. Some previous reports indicate that leptin administration increases a marker of leptin signal transduction (pSTAT) in *Pomc*^{eGFP} cells (45), thereby providing evidence of co-localization. To facilitate the visualization of POMC and LepRb cells and to quantify co-expression, we crossed *LepRb*^{tDTomato} mice with *Pomc*^{eGFP} mice to create a double reporter line (*Pomc*^{eGFP}:*LepRb*^{tdTomato}). We found that 20.6% ± 2.14 of POMC^{NTS} cells co-localized with LepRb^{tdTomato} (Fig. 2I). Co-localization was highest at -7.64 and -7.76 from bregma, the subregion of the NTS we found to express the majority of POMC cells (Fig. 1C). All *Pomc*^{eGFP} cells co-expressed Phox2b, a transcription factor associated with the formation and development of the NTS (74) (Fig. 2J). Using *LepRb*$^{CRE:eGFP}$ mice to visualize LepRb^{NTS} expression, we observed that all LepRb^{NTS} cells also expressed Phox2b (Fig. 2K and 2L).

Pomc^{eGFP} cells increase their activity in response to food intake

Given that a subset of POMC^{NTS} cells co-express LepRb, we postulated that this subgroup should be responsive to leptin. Fasting has been shown to affect the concentrations of various circulating hormones, including reducing leptin (75). We dark cycle fasted mice, dark cycle fasted and then re-fed mice, or ad libitum fed mice and measured serum leptin and the activity of POMC^{NTS} cells using FOS-IR (Fig. 3). The NTS and blood was collected 2 to 4 hours following the onset of the light cycle. As expected, fasting significantly reduced leptin levels (0.56 ± 0.30 ng/ml, n = 4) and fasting followed by a 2-hour bout of refeeding significantly increased leptin levels (3.44 ± 0.82 ng/ml, n = 8; $F_{2,19} = 4.64$, $P = 0.023$; Fig. 3E). A significant difference in leptin levels between the refed group and the fed group (1.58 ± 0.32 ng/ml, n = 9) was not detected. Refeeding (n = 9) also significantly increased the number of FOS-IR-positive cells within the NTS compared to the fasted state or fed state (Fig. 3E). Significantly more NTS *Pomc*^{eGFP} neurons expressed FOS-IR in mice that had been fasted and then refed (21.34 ± 6.91 cells) compared to mice in the fasted (0.93 ± 0.42 cells) or fed state (1.29 ± 0.54 cells; $F_{2,11} = 7.55$, $P = 0.008$, n = 4–5 per group; Fig. 3A–3D). These findings suggest that a subset of POMC^{NTS} cells are responsive to nutritional state and changes in hormones such as endogenous leptin levels.

Leptin activates a subset of POMC^{NTS} neurons

To gain further insight into the physiological role of the LepRb expression on POMC^{NTS} cell activity, we examined the effect of peripheral administration of leptin. Consistent with the fluctuations of endogenous leptin described above, we observed that leptin (5 mg/kg, i.p.) increased FOS-IR within the NTS compared to saline treatment (Fig. 4A). We examined the effect specifically in POMC^{NTS} cells and found that leptin increased

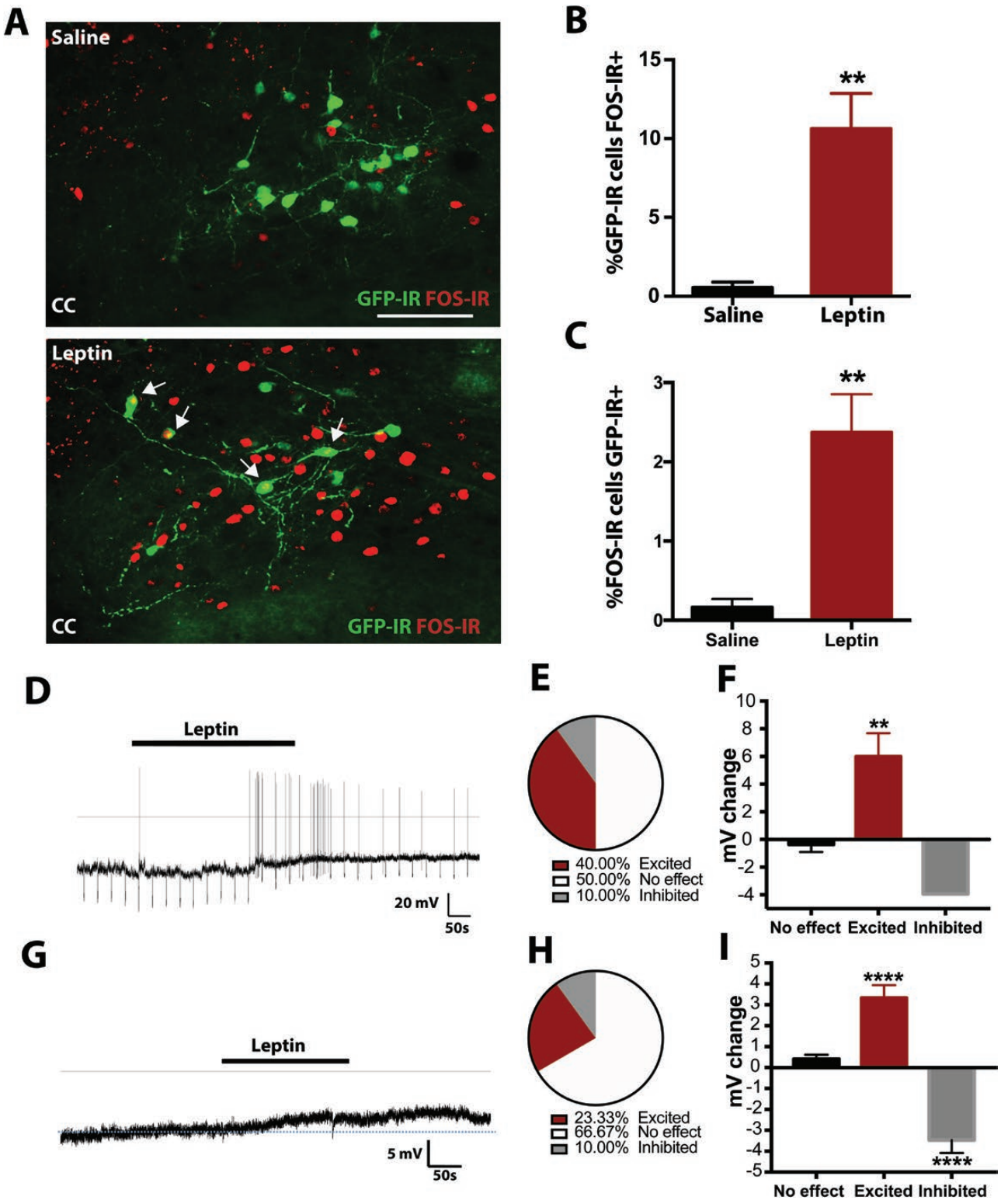

Figure 4. *Pomc*^{eGFP} cells are responsive to changes in exogenous leptin levels. **A–C:** Leptin treatment (5 mg/kg, i.p.) in *Pomc*^{eGFP} mice increased FOS-IR within GFP-IR **(A–B)** and non-GFP-IR NTS cells **(C)** compared to saline treatment (n = 10). Level of NTS presented in A, -7.56 to -7.76 from bregma. **D:** Representative current clamp recording of a *Pomc*^{eGFP} cell. **E–F:** Bath application of leptin (100–250 nM) increased the membrane potential of 4 out of 10 *Pomc*^{eGFP} cells and reduced the membrane potential of 1 cell. **G:** Representative current clamp recording of a *Pomc*^{eGFP} cell in the presence of synaptic blockers (1 µM tetrodotoxin, 3 µM strychnine, 50 µM picrotoxin, 50 µM D-AP5, 10 µM CNQX). **H–I:** Bath application of leptin (250–500 nM) depolarised and increased the membrane potential of 7 of 30 *Pomc*^{eGFP} cells and inhibitory effects were observed in 3 cells. Arrows represent dual-labeled cells. CC, central canal; scale bar A, 50 µm. Data are presented as mean ± SEM. ** $P < 0.01$, **** $P < 0.0001$.

FOS-IR within POMC-eGFP-IR cells compared with saline ($t(8) = 4.44$, $P = 0.001$, n = 5 per group; Fig. 4B). However, leptin also increased FOS-IR in chemically undefined NTS cell populations. Only 2.37% of FOS-IR-positive cells were POMC-eGFP-IR (Fig. 4C).

To examine the leptin-associated activation of POMC-eGFP-IR cells further, we measured the effect of leptin on the electrical activity of $POMC^{NTS}$ cells ex vivo. Bath application of leptin (100–250 nM) increased the firing rate of 40% of POMC neurons (6.00 ± 1.67 mV vs. -0.36 ± 0.55 mV, $t(8) = 3.98$, $P = 0.005$, n = 4/10 cells; Fig. 4D–4F). This effect was postsynaptic, as the depolarization persisted in the presence of synaptic blockers (3.33 ± 0.61 mV vs. -0.41 ± 0.20 mV, $F_{2,27} = 41.61$, $P < 0.0001$, n = 7/30 cells; Fig. 4G–4I). The in vivo and ex vivo data highlight that a subset of $Pomc^{eGFP}$ neurons in the NTS respond to leptin.

Discussion

Obesity has emerged as a key challenge to human health, making it essential that the neurobiology underpinning energy homeostasis is clarified to foster the identification of new strategies to prevent and treat this condition. Genetic analysis has revealed that a functioning melanocortin system is necessary for healthy body weight in multiple species. Specifically, genetic disruption of *POMC/Pomc* and *MC4R/Mc4r* promotes severe hyperphagia and obesity (76). Within the adult brain POMC is predominantly expressed within the ARC, and the function of $POMC^{ARC}$ has been extensively characterized. Here we investigated the smaller and less well-studied population within the NTS.

Distribution of $POMC^{NTS}$

Low levels of endogenous *Pomc* expression within the NTS have hampered the study of this subpopulation. To overcome these technical restrictions, we utilized a reporter mouse line that allowed us to map, quantify, and characterize these cells. Here we provide an instrumental validation of the expression of endogenous *Pomc* mRNA in eGFP cells in the $Pomc^{eGFP}$ mouse line. We report that $POMC^{NTS}$ cells are primarily localized within the commissural NTS at the level of the AP. Though other energy balance modulating neurons are present within the caudal DVC, we observed a lack of co-localisation with CCK, GLP-1, TH, BDNF, nesfatin, nNOS, seipin, or ChAT-containing cells. $POMC^{NTS}$ cells are activated by visceral afferents and chemogenetic activation of $POMC^{NTS}$ decreases acute food intake and produces opioid analgesia and bradycardia (30, 36, 77). This suggests that $POMC^{NTS}$ cells may constitute a distinct hub within the hindbrain for the regulation of food intake via peptide product α-MSH and for the induction of analgesia via peptide product β-endorphin. The melanocortin system also appears to play a role in blood pressure and heart rate. Compared to equally obese control subjects, the prevalence of hypertension in MC4R-deficient people was significantly lower, and MC4R-deficient patients exhibited lower increases in heart rate upon waking (78). Though lacking direct co-expression, $POMC^{NTS}$ cells may form local interactions with neighboring DVC TH, GLP-1, CCK, BDNF, nesfatin, nNOS, seipin, and/or ChAT cells to impact homeostasis, analgesia, and/or blood pressure.

In support of system connectivity, CCK increases the firing rate of $POMC^{NTS}$ cells (30). Though CCK is widely expressed within the CNS, recent reports support a functional role of the subpopulation of CCK-positive neurons within the NTS in feeding behavior and body weight regulation. Specifically, chemogenetic or optogenetic activation of CCK^{NTS} neurons potently reduces food intake and body weight (38, 39). This effect appears to be mediated via transmitter release in the paraventricular nucleus of the hypothalamus (PVH) and parabrachial nucleus (PBN) given that selective optogenetic activation of CCK^{NTS} axon terminals within these regions reduces feeding (38, 39). A subset of CCK^{NTS} cells co-express PPG/GLP-1 (43). Like CCK^{NTS}, chemogenetic activation of $PPG/GLP\text{-}1^{NTS}$ cells also suppresses acute feeding (41).

Nesfatin-1 is a peptide and neuropeptide first identified in 2006 and observed to reduce food intake (79). $Nesfatin^{NTS}$ cells are responsive to CCK-8 and gastric distention (80–82). It is therefore possible that CCK^{NTS} not only impacts feeding via a PVH and PBN circuit, but also via a local interaction with nesfatin and POMC. Providing support for potential cardiovascular function, NTS microinfusion of nesfatin-1 increases blood pressure and heart rate (80). A subset of $Nesfatin^{NTS}$ cells co-express GABA and the majority of the dorsal motor nucleus of the vagus (DMX) nesfatin cells co-express ChAT. $Nesfatin^{DMX}$ cells innervate the stomach (80).

One of the best described cell types within the NTS modulating feeding behavior are those expressing the catecholamines. Similar to our findings, Fan and colleagues reported no overlap between the expression of POMC and TH in the NTS (31). Like $POMC^{NTS}$ cells, vagal afferents also directly innervate TH^{NTS} cells (83) and similar to $nestfatin^{NTS}$, TH^{NTS} are responsive to gastric distension (84). Direct chemogenetic or optogenetic activation of noradrenergic dopamine β-hydroxylase (DBH)-expressing NTS neurons also decreases food intake and body weight (39). Supporting a cardiovascular function, DBH conjugated to the neurotoxin saporin,

but not the neurotoxin 6-hydroxydopamine (6-OHDA) infused into the NTS, causes myocardial lesions and in some cases sudden death (85, 86).

As observed in *POMC* deficiency, genetic alterations in *BDNF* in humans is linked to elevated food intake and obesity (87, 88). BDNF function is best characterized within the ventromedial hypothalamus (VMH) (89). BDNF signaling within the NTS is essential to life, as the knockout of its receptor TrkB within the NTS is lethal (90). Heterozygous mice with partial knockdown are hyperphagic but display a normal body weight (90). Additional research is required to define a function for $BDNF^{NTS}$.

Despite being known primarily for its role in adipocyte differentiation, the protein seipin is expressed within the NTS; however, its function within this region has yet to be fully explored (62). nNOS plays a role in a variety of processes, including blood pressure, energy homeostasis, and synaptic plasticity. Viral knockdown of $nNOS^{NTS}$ in rats inhibited sympathetically mediated baroreflex (91), though food intake and body weight in these rats was not reported and remains to be investigated. Thus, the NTS harbors a variety of factors involved in homeostatic regulation and future study is warranted to unpick potential local interactions and their functional implications.

Though $POMC^{NTS}$ cells do not co-express CCK, GLP-1, TH, BDNF, nesfatin, seipin, or nNOS, 100% of $POMC^{NTS}$ co-express Phox2b. Phox2b is a transcription factor that is required for the embryonic development of the autonomic nervous system. The $Phox2b^{CRE}$ line is frequently used as a broad NTS histochemical marker or to genetically alter cells within the NTS. Functionally, subsets of Phox2b cells have been reported to be involved in central excitatory relays of the sympathetic baroreflex and transmit peripheral chemoreceptor information to the retrotrapezoid nucleus (92, 93). Moreover, a recent study revealed that a subset of $Phox2b^{NTS}$ neurons act as central respiratory chemoreceptors (94).

Modulation of $POMC^{NTS}$

In line with previous findings (31), we observed that the activity (as detected by FOS-IR) of a small subset of POMC-$eGFP^{NTS}$ cells is activated by a feeding bout. In the present report, we employed an acute fast followed by 2 hours of refeeding. In the earlier report, $Pomc^{eGFP}$ mice were on a restricted feeding schedule of 5 hours per day (31). The proportion of $POMC^{NTS}$ cells activated following refeeding was greater than that observed in response to leptin treatment, suggesting that other homeostatic factors modulate the activity of $POMC^{NTS}$ cells. We found that $POMC^{NTS}$ cells expressing LepRbs were primarily concentrated -7.56 to -7.92 from bregma, an area where POMC neurons have been shown to respond to dietary amino acids (95, 96). A study by Grill and colleagues provides support that LepRbs within the NTS are required for appropriate energy homeostasis (97). Specifically, they observed that viral knockdown of LepRb within the NTS increased food intake, body weight, and adiposity in rats. $Phox2b^{CRE}$:$LepRb^{flox'd}$ mice were hyperphagic, displayed increased food intake after fasting, and gained weight at a faster rate than wild-type controls. $Phox2b^{CRE}$:$LepRb^{flox'd}$ mice also exhibited an increased metabolic rate independent of changes in locomotor activity and normal glucose homeostasis (98). These data suggest that leptin signaling within the NTS is required for normal feeding and body weight in rodents and that a subset of $POMC^{NTS}$ cells are regulated by leptin.

In line with other earlier work, we observed increased FOS-IR in a subpopulation of $POMC^{NTS}$ cells following acute leptin treatment (45, 99). However, our results do not coincide with similar experiments utilising a $Pomc^{CRE}$-driven reporter line (46). As the $Pomc^{eGFP}$ and the $Pomc^{CRE}$ reporter lines appear to label nonoverlapping neuronal populations within the NTS (8), it is likely that the cells characterized here and in references 45 and 99 represent a different population to those studied in reference 46. To further investigate the mechanism by which $POMC^{NTS}$ neurons respond to leptin, we employed whole cell patch clamp electrophysiology. Leptin's effects on neuronal excitability in the rat brainstem are varied and appear to encompass cells that are inhibited, excited, or nonresponsive (100, 101). Approximately half of the unidentified neurons described in these studies became hyperpolarized upon leptin application, while a smaller proportion (13%) showed an increase in membrane potential (100, 101). We provide some of the first insights into the effect of leptin on $Pomc^{eGFP}$ cells. We found that leptin increased the firing rate of approximately a quarter of $Pomc^{eGFP}$ cells, a pattern similar to the proportion of $POMC^{NTS}$ FOS-IR-positive cells. As the membrane potential increase endured in the presence of synaptic blockers, we conclude that $POMC^{NTS}$ cells possess the required cellular machinery to respond directly to circulating levels of this hormone. However, the effects observed were small and warrant further investigation with different concentrations of leptin and different electrophysiological techniques to further clarify both the network and direct effects of leptin on $Pomc^{eGFP}$ cell activity. TRPC channels are responsible for the activation of $POMC^{ARC}$ neurons by leptin (102). The precise electrophysiological mechanism and the current responsible for $POMC^{NTS}$ effects also remain to be elucidated.

We recently reported that approximately 40% of $POMC^{NTS}$ cells co-express the 2c receptor subtype for the neurotransmitter serotonin ($5\text{-}HT_{2C}R$) (37). Moreover, we observed that $POMC^{NTS}$ is essential for the appetite suppressive effects of the $5\text{-}HT_{2C}R$ obesity medication lorcaserin (37). The findings reported here add to the profile of $POMC^{NTS}$ and its potential physiological role. Specifically, we dissect the interplay of 2 of the most essential players in body weight regulation, the melanocortin and leptin systems, within the key homeostatic brain region the NTS. We reveal that $POMC^{NTS}$ cells represent a segregated class of leptin responsive neurons that do not co-localize other established NTS metabolic regulators. These findings provide new insights into the neuroendocrinology of appetite and have implications for the neurobiology of obesity.

Financial Support: Work was supported by the Wellcome Trust (WT081713, WT098012 and 204815/Z/16/Z to LKH; 093566/Z/10/A to LKH/LKB), the Biotechnology and Biological Sciences Research Council (BB/K001418/1, BB/NO17838/1 to LKH), and the Medical Research Council (MRC; MC/PC/15077 to LKH). The Genomics and Transcriptomics Core facility utilized was supported by the MRC (MRC_MC_UU_12012/5) and Wellcome Trust (100574/Z/12/Z).

Additional Information

Correspondence: L.K. Heisler, Rowett Institute, University of Aberdeen, Foresterhill, Aberdeen, AB25 2ZD, UK. E-mail: lora.heisler@abdn.ac.uk.

Disclosure Summary: The authors have nothing to disclose.

References

1. Harno E, Gali Ramamoorthy T, Coll AP, White A. POMC: the physiological power of hormone processing. *Physiol Rev*. 2018;**98**(4):2381–2430.
2. Garfield AS, Lam DD, Marston OJ, Przydzial MJ, Heisler LK. Role of central melanocortin pathways in energy homeostasis. *Trends Endocrinol Metab*. 2009;**20**(5):203–215.
3. Butler AA, Marks DL, Fan W, Kuhn CM, Bartolome M, Cone RD. Melanocortin-4 receptor is required for acute homeostatic responses to increased dietary fat. *Nat Neurosci*. 2001;**4**(6):605–611.
4. Fan W, Dinulescu DM, Butler AA, Zhou J, Marks DL, Cone RD. The central melanocortin system can directly regulate serum insulin levels. *Endocrinology*. 2000;**141**(9):3072–3079.
5. Huszar D, Lynch CA, Fairchild-Huntress V, et al. Targeted disruption of the melanocortin-4 receptor results in obesity in mice. *Cell*. 1997;**88**(1):131–141.
6. Joseph SA, Pilcher WH, Benneti C. Immunocytochemical localization of ACTH parikarya in nucleus tractus solitarius: evidence for a second opiocortin neuronal system. *Neurosci Lett*. 1983;**38**(3):221–225.
7. Paikovlts M. Pro-opiomelanocortin-derived peptides (ACTH/β-endorphin/α-MSH) in brainstem baroreceptor areas of the rat. *Brain Res*. 1987;**436**(2):323–338.
8. Padilla SL, Reef D, Zeltser LM. Defining POMC neurons using transgenic reagents: impact of transient Pomc expression in diverse immature neuronal populations. *Endocrinology*. 2012;**153**(3):1219–1231.
9. Padilla SL, Carmody JS, Zeltser LM. Pomc-expressing progenitors give rise to antagonistic neuronal populations in hypothalamic feeding circuits. *Nat Med*. 2010;**16**(4):403–405.
10. Obici S, Feng Z, Tan J, Liu L, Karkanias G, Rossetti L. Central melanocortin receptors regulate insulin action. *J Clin Invest*. 2001;**108**(7):1079–1085.
11. Fan W, Boston BA, Kesterson RA, Hruby VJ, Cone RD. Role of melanocortinergic neurons in feeding and the agouti obesity syndrome. *Nature*. 1997;**385**(6612):165–168.
12. Pierroz DD, Ziotopoulou M, Ungsunan L, Moschos S, Flier JS, Mantzoros CS. Effects of acute and chronic administration of the melanocortin agonist MTII in mice with diet-induced obesity. *Diabetes*. 2002;**51**(5):1337–1345.
13. Challis BG, Coll AP, Yeo GSH, et al. Mice lacking pro-opiomelanocortin are sensitive to high-fat feeding but respond normally to the acute anorectic effects of peptide-$YY_{3–36}$. *Proc Natl Acad Sci U S A*. 2004;**101**(13):4695–4700.
14. Coll AP, Loraine Tung YC. Pro-opiomelanocortin (POMC)-derived peptides and the regulation of energy homeostasis. *Mol Cell Endocrinol*. 2009;**300**(1-2):147–151.
15. Farooqi S, Keogh JM, Yeo GSH, Lank EJ, Cheetham T, O'Rahilly S. Clinical spectrum of obesity and mutations in the melanocortin 4 receptor gene. *N Engl J Med*. 2003;**348**(12):1085–1095.
16. Farooqi IS, O'Rahilly S. Mutations in ligands and receptors of the leptin-melanocortin pathway that lead to obesity. *Nat Clin Pract Endocrinol Metab*. 2008;**4**(10):569–577.
17. Hinney A, Schmidt A, Nottebom K, et al. Several mutations in the melanocortin-4 receptor gene including a nonsense and a frameshift mutation associated with dominantly inherited obesity in humans. *J Clin Endocrinol Metab*. 1999;**84**(4):1483–1486.
18. Lee YS, Challis BG, Thompson DA, et al. A POMC variant implicates beta-melanocyte-stimulating hormone in the control of human energy balance. *Cell Metab*. 2006;**3**(2):135–140.
19. Yaswen L, Diehl N, Brennan MB, Hochgeschwender U. Obesity in the mouse model of pro-opiomelanocortin deficiency responds to peripheral melanocortin. *Nat Med*. 1999;**5**(9):1066–1070.
20. Yen TT, Gill AM, Frigeri LG, Barsh GS, Wolff GL. Obesity, diabetes, and neoplasia in yellow A(vy)/- mice: ectopic expression of the agouti gene. *Faseb J*. 1994;**8**(8):479–488.
21. Yeo GS, Farooqi IS, Aminian S, Halsall DJ, Stanhope RG, O'Rahilly S. A frameshift mutation in MC4R associated with dominantly inherited human obesity. *Nat Genet*. 1998;**20**(2):111–112.
22. Song Y, Cone RD. Creation of a genetic model of obesity in a teleost. *Faseb J*. 2007;**21**(9):2042–2049.
23. Raffan E, Dennis RJ, O'Donovan CJ, et al. A deletion in the canine POMC gene is associated with weight and appetite in obesity-prone labrador retriever dogs. *Cell Metab*. 2016;**23**(5):893–900.
24. Coll AP, Farooqi IS, Challis BG, Yeo GS, O'Rahilly S. Proopiomelanocortin and energy balance: insights from human and murine genetics. *J Clin Endocrinol Metab*. 2004;**89**(6):2557–2562.
25. Tung YC, Rimmington D, O'Rahilly S, Coll AP. Pro-opiomelanocortin modulates the thermogenic and physical activity responses to high-fat feeding and markedly influences dietary fat preference. *Endocrinology*. 2007;**148**(11):5331–5338.
26. Cone RD. Anatomy and regulation of the central melanocortin system. *Nat Neurosci*. 2005;**8**(5):571–578.
27. Burke LK, Heisler LK. 5-hydroxytryptamine medications for the treatment of obesity. *J Neuroendocrinol*. 2015;**27**(6):389–398.
28. Williams KW, Elmquist JK. From neuroanatomy to behavior: central integration of peripheral signals regulating feeding behavior. *Nat Neurosci*. 2012;**15**(10):1350–1355.
29. Heisler LK, Lam DD. An appetite for life: brain regulation of hunger and satiety. *Curr Opin Pharmacol*. 2017;**37**(Dec):100–106.

30. Appleyard SM, Bailey TW, Doyle MW, et al. Proopiomelanocortin neurons in nucleus tractus solitarius are activated by visceral afferents: regulation by cholecystokinin and opioids. *J Neurosci*. 2005;**25**(14):3578–3585.
31. Fan W, Ellacott KL, Halatchev IG, Takahashi K, Yu P, Cone RD. Cholecystokinin-mediated suppression of feeding involves the brainstem melanocortin system. *Nat Neurosci*. 2004;**7**(4):335–336.
32. Hisadome K, Reimann F, Gribble FM, Trapp S. Leptin Directly Depolarizes Preproglucagon Neurons in the Nucleus Tractus Solitarius Electrical Properties of Glucagon-Like Peptide 1 Neurons. *Diabetes*. 2010;**59**(8):1890–1898.
33. Hisadome K, Reimann F, Gribble FM, Trapp S. CCK stimulation of GLP-1 neurons involves α1-adrenoceptor-mediated increase in glutamatergic synaptic inputs. *Diabetes*. 2011;**60**(11):2701–2709.
34. Ellacott KL, Halatchev IG, Cone RD. Interactions between gut peptides and the central melanocortin system in the regulation of energy homeostasis. *Peptides*. 2006;**27**(2):340–349.
35. Blouet C, Schwartz GJ. Brainstem nutrient sensing in the nucleus of the solitary tract inhibits feeding. *Cell Metab*. 2012;**16**(5):579–587.
36. Zhan C, Zhou J, Feng Q, et al. Acute and long-term suppression of feeding behavior by POMC neurons in the brainstem and hypothalamus, respectively. *J Neurosci*. 2013;**33**(8):3624–3632.
37. D'Agostino G, Lyons D, Cristiano C, et al. Nucleus of the solitary tract serotonin 5-HT2C receptors modulate food intake. *Cell Metab*. 2018;**28**(4):619–630.e5.
38. D'Agostino G, Lyons DJ, Cristiano C, et al. Appetite controlled by a cholecystokinin nucleus of the solitary tract to hypothalamus neurocircuit. *Elife*. 2016;**5**(March):1–15.
39. Roman CW, Derkach VA, Palmiter RD. Genetically and functionally defined NTS to PBN brain circuits mediating anorexia. *Nat Commun*. 2016;**7**(May):11905.
40. Cork SC, Richards JE, Holt MK, Gribble FM, Reimann F, Trapp S. Distribution and characterisation of Glucagon-like peptide-1 receptor expressing cells in the mouse brain. *Mol Metab*. 2015;**4**(10):718–731.
41. Holt MK, Richards JE, Cook DR, et al. Preproglucagon neurons in the nucleus of the solitary tract are the main source of brain GLP-1, mediate stress-induced hypophagia, and limit unusually large intakes of food. *Diabetes*. 2019;**68**(1):21–33.
42. Ritter S, Bugarith K, Dinh TT. Immunotoxic destruction of distinct catecholamine subgroups produces selective impairment of glucoregulatory responses and neuronal activation. *J Comp Neurol*. 2001;**432**(2):197–216.
43. Garfield AS, Patterson C, Skora S, et al. Neurochemical characterization of body weight-regulating leptin receptor neurons in the nucleus of the solitary tract. *Endocrinology*. 2012;**153**(10):4600–4607.
44. Brailoiu GC, Dun SL, Brailoiu E, et al. Nesfatin-1: distribution and interaction with a G protein-coupled receptor in the rat brain. *Endocrinology*. 2007;**148**(10):5088–5094.
45. Ellacott KL, Halatchev IG, Cone RD. Characterization of leptin-responsive neurons in the caudal brainstem. *Endocrinology*. 2006;**147**(7):3190–3195.
46. Huo L, Grill HJ, Bjørbaek C. Divergent regulation of proopiomelanocortin neurons by leptin in the nucleus of the solitary tract and in the arcuate hypothalamic nucleus. *Diabetes*. 2006;**55**(3):567–573.
47. Cohen P, Zhao C, Cai X, et al. Selective deletion of leptin receptor in neurons leads to obesity. *J Clin Invest*. 2001;**108**(8):1113–1121.
48. Farooqi IS, Wangensteen T, Collins S, et al. Clinical and molecular genetic spectrum of congenital deficiency of the leptin receptor. *N Engl J Med*. 2007;**356**(3):237–247.
49. Elmquist JK, Elias CF, Saper CB. From lesions to leptin: hypothalamic control of food intake and body weight. *Neuron*. 1999;**22**(2):221–232.
50. Balthasar N, Coppari R, McMinn J, et al. Leptin receptor signaling in POMC neurons is required for normal body weight homeostasis. *Neuron*. 2004;**42**(6):983–991.
51. Rupp AC, Allison MB, Jones JC, et al. Specific subpopulations of hypothalamic leptin receptor-expressing neurons mediate the effects of early developmental leptin receptor deletion on energy balance. *Mol Metab*. 2018;**14**(Aug):130–138.
52. Cowley MA, Smart JL, Rubinstein M, et al. Leptin activates anorexigenic POMC neurons through a neural network in the arcuate nucleus. *Nature*. 2001;**411**(6836):480–484.
53. Leinninger GM, Jo YH, Leshan RL, et al. Leptin acts via leptin receptor-expressing lateral hypothalamic neurons to modulate the mesolimbic dopamine system and suppress feeding. *Cell Metab*. 2009;**10**(2):89–98.
54. Scott MM, Lachey JL, Sternson SM, et al. Leptin targets in the mouse brain. *J Comp Neurol*. 2009;**514**(5):518–532.
55. *RRID: AB_300798*. https://scicrunch.org/resolver/AB_300798.
56. *RRID: AB_2614470*. https://scicrunch.org/resolver/AB_2614470.
57. *RRID: AB_2737429*. https://scicrunch.org/resolver/AB_2737429.
58. *RRID:AB_390204*. https://scicrunch.org/resolver/AB_390204.
59. *RRID: AB_2079751*. https://scicrunch.org/resolver/AB_2079751.
60. *RRID: AB_572255*. https://scicrunch.org/resolver/AB_572255.
61. Ito D, Suzuki N. Molecular pathogenesis of seipin/BSCL2-related motor neuron diseases. *Ann Neurol*. 2007;**61**(3):237–250.
62. Garfield AS, Chan WS, Dennis RJ, Ito D, Heisler LK, Rochford JJ. Neuroanatomical characterisation of the expression of the lipodystrophy and motor-neuropathy gene Bscl2 in adult mouse brain. *Plos One*. 2012;**7**(9):e45790.
63. *RRID: AB_2819210*. https://scicrunch.org/resolver/AB_2819210.
64. *RRID: AB_10675986*. https://scicrunch.org/resolver/AB_10675986.
65. *RRID: AB_2340375*. https://scicrunch.org/resolver/AB_2340375.
66. *RRID: AB_141637*. https://scicrunch.org/resolver/AB_141637.
67. *RRID: AB_141633*. https://scicrunch.org/resolver/AB_141633.
68. *RRID: AB_142540*. https://scicrunch.org/resolver/AB_142540.
69. Paxinos G, Franklin KBJ. The mouse brain in stereotaxic coordinates - Third Edition. *Acad Press*. 2008;**94**(C9):1–350. papers2://publication/uuid/06D6DDC2-9CE7-4765-8202-DDA77733788C.
70. *RRID: AB_2106755*. https://scicrunch.org/resolver/AB_2106755.
71. *RRID: AB_2340593*. https://scicrunch.org/resolver/AB_2340593.
72. *RRID: AB_304897*. https://scicrunch.org/resolver/AB_304897.
73. *RRID: AB_2336126*. https://scicrunch.org/resolver/AB_2336126.
74. Dauger S, Pattyn A, Lofaso F, et al. Phox2b controls the development of peripheral chemoreceptors and afferent visceral pathways. *Development*. 2003;**130**(26):6635–6642.
75. Boelen A, Kwakkel J, Vos XG, Wiersinga WM, Fliers E. Differential effects of leptin and refeeding on the fasting-induced decrease of pituitary type 2 deiodinase and thyroid hormone receptor beta2 mRNA expression in mice. *J Endocrinol*. 2006;**190**(2):537–544.
76. Yeo GS, Heisler LK. Unraveling the brain regulation of appetite: lessons from genetics. *Nat Neurosci*. 2012;**15**(10):1343–1349.
77. Cerritelli S, Hirschberg S, Hill R, Balthasar N, Pickering AE. Activation of brainstem pro-opiomelanocortin neurons produces opioidergic analgesia, bradycardia and bradypnoea. *Plos One*. 2016;**11**(4):e0153187.
78. Greenfield JR, Miller JW, Keogh JM, et al. Modulation of blood pressure by central melanocortinergic pathways. *N Engl J Med*. 2009;**360**(1):44–52.
79. Oh-I S, Shimizu H, Satoh T, et al. Identification of nesfatin-1 as a satiety molecule in the hypothalamus. *Nature*. 2006;**443**(*7112*):709–712.
80. Bonnet MS, Ouelaa W, Tillement V, et al. Gastric distension activates NUCB2/nesfatin-1-expressing neurons in the nucleus of the solitary tract. *Regul Pept*. 2013;**187**(Nov):17–23.
81. Stengel A, Goebel M, Wang L, et al. Central nesfatin-1 reduces dark-phase food intake and gastric emptying in rats: Differential role of corticotropin-releasing factor2 receptor. *Endocrinology*. 2009;**150**(11):4911–4919.
82. Noetzel S, Stengel A, Inhoff T, et al. CCK-8S activates c-Fos in a dose-dependent manner in nesfatin-1 immunoreactive neurons in the paraventricular nucleus of the hypothalamus and in

the nucleus of the solitary tract of the brainstem. *Regul Pept*. 2009;**157**(1-3):84–91.
83. Appleyard SM, Marks D, Kobayashi K, Okano H, Low MJ, Andresen MC. Visceral afferents directly activate catecholamine neurons in the solitary tract nucleus. *J Neurosci*. 2007;**27**(48):13292–13302.
84. Rinaman L, Baker EA, Hoffman GE, Stricker EM, Verbalis JG. Medullary c-Fos activation in rats after ingestion of a satiating meal. *Am J Physiol Integr Comp Physiol*. 2017;**275**(1):R262–R268.
85. Talman WT, Dragon DN, Jones SY, Moore SA, Lin LH. Sudden death and myocardial lesions after damage to catecholamine neurons of the nucleus tractus solitarii in rat. *Cell Mol Neurobiol*. 2012;**32**(7):1119–1126.
86. Talman WT, Lin LH. Sudden death following selective neuronal lesions in the rat nucleus tractus solitarii. *Auton Neurosci*. 2013;**175**(1-2):9–16.
87. Gray J, Yeo GS, Cox JJ, et al. Hyperphagia, severe obesity, impaired cognitive function, and hyperactivity associated with functional loss of one copy of the brain-derived neurotrophic factor (BDNF) gene. *Diabetes*. 2006;**55**(12):3366–3371.
88. Han JC, Liu QR, Jones M, et al. Brain-derived neurotrophic factor and obesity in the WAGR syndrome. *N Engl J Med*. 2008;**359**(9):918–927.
89. Unger TJ, Calderon GA, Bradley LC, Sena-Esteves M, Rios M. Selective deletion of Bdnf in the ventromedial and dorsomedial hypothalamus of adult mice results in hyperphagic behavior and obesity. *J Neurosci*. 2007;**27**(52):14265–14274.
90. Ozek C, Zimmer DJ, De Jonghe BC, Kalb RG, Bence KK. Ablation of intact hypothalamic and/or hindbrain TrkB signaling leads to perturbations in energy balance. *Mol Metab*. 2015;**4**(11):867–880.
91. Lin LH, Nitschke Dragon D, Jin J, et al. Decreased expression of neuronal nitric oxide synthase in the nucleus tractus solitarii inhibits sympathetically mediated baroreflex responses in rat. *J Physiol*. 2012;**590**(15):3545–3559.
92. Kang BJ, Chang DA, Mackay DD, et al. Central nervous system distribution of the transcription factor Phox2b in the adult rat. *J Comp Neurol*. 2007;**503**(5):627–641.
93. Stornetta RL, Moreira TS, Takakura AC, et al. Expression of Phox2b by brainstem neurons involved in chemosensory integration in the adult rat. *J Neurosci*. 2006;**26**(40):10305–10314.
94. Fu C, Shi L, Wei Z, et al. Activation of Phox2b-expressing neurons in the nucleus tractus solitarii drives breathing in mice. *J Neurosci*. 2019;**39**(15):2837–2846.
95. Yamamoto T, Sawa K. Comparison of c-fos-like immunoreactivity in the brainstem following intraoral and intragastric infusions of chemical solutions in rats. *Brain Res*. 2000;**866**(1-2):144–151.
96. Schwarz J, Burguet J, Rampin O, et al. Three-dimensional macronutrient-associated Fos expression patterns in the mouse brainstem. *Plos One*. 2010;**5**(2):e8974.
97. Hayes MR, Skibicka KP, Leichner TM, et al. Endogenous leptin signaling in the caudal nucleus tractus solitarius and area postrema is required for energy balance regulation. *Cell Metab*. 2010;**11**(1):77–83.
98. Scott MM, Williams KW, Rossi J, Lee CE, Elmquist JK. Leptin receptor expression in hindbrain Glp-1 neurons regulates food intake and energy balance in mice. *J Clin Invest*. 2011;**121**(6):2413–2421.
99. Lam DD, Attard CA, Mercer AJ, Myers MG Jr, Rubinstein M, Low MJ. Conditional expression of Pomc in the Leprpositive subpopulation of POMC neurons is sufficient for normal energy homeostasis and metabolism. *Endocrinology*. 2015;**156**(4):1292–1302.
100. Williams KW, Smith BN. Rapid inhibition of neural excitability in the nucleus tractus solitarii by leptin: implications for ingestive behaviour. *J Physiol*. 2006;**573**(Pt 2):395–412.
101. Williams KW, Zsombok A, Smith BN. Rapid inhibition of neurons in the dorsal motor nucleus of the vagus by leptin. *Endocrinology*. 2007;**148**(4):1868–1881.
102. Qiu J, Fang Y, Rønnekleiv OK, Kelly MJ. Leptin excites proopiomelanocortin neurons via activation of TRPC channels. *J Neurosci*. 2010;**30**(4):1560–1565.